The Formation and Fate of a River Plume: A Numerical Model

JAMES O'DONNELL

Department of Marine Sciences, The University of Connecticut, Groton, Connecticut

(Manuscript received 24 March 1989, in final form 30 October 1989)

ABSTRACT

A mathematical model that describes the formation and dilution of a frontally bounded river plume is presented. Such features were first studied at the mouth of the Connecticut River during periods of high discharge and have subsequently been reported elsewhere. The model incorporates the effects of nonlinear advection, Coriolis acceleration, time dependency, mixing, friction, and a free frontal boundary. A numerical solution technique is employed to obtain approximate solutions to several problems which are interpreted to yield new insights to the dynamics of these phenomena.

In particular, computed solutions for the growth of a plume discharged from a radial source into a steady crossflow are presented for a variety of crossflow velocities and physical scales. These demonstrate that the stability of the layer to vertical shear in the horizontal velocity is sensitive to the relative directions of the crossflow current and that of a free Kelvin wave. The effect of a reversing crossflow, representative of a tidal current, is therefore of interest and calculations indicate that river plumes, like that of the Connecticut River, are diluted by vertical mixing soon after the times of high and low water. This conclusion is of obvious ecological importance.

1. Introduction

Thin surface layers of buoyant water attributable to river discharges are ubiquitous in coastal oceans and estuaries, often dominating the local physical and biological processes. These plumes of brackish water have been observed to occur on a large range of scales extending from $O(10^2$ m) at the mouth of the Leschenault Estuary, Luketina and Imberger (1987), to $O(10^5$ m) at the mouth of the Yangtze River, Beardsley et al. (1985). Unsteady behavior has also been noted and associated with tidal motion in ambient receiving basins and direct wind forcing. Obviously, these flows encompass a wide variety of dynamic regimes and, in contrast to previous work on plume dynamics, this paper presents the results of an investigation of a theoretical model of the unsteady behavior of small scale river plumes in which the influence of planetary rotation, as estimated by comparing the characteristic plume scale to the internal Rossby deformation radius, is of secondary influence.

Another unusual feature of this model, is the explicit description of the frontal boundary that has been found to partially surround many small plumes and which were first reported by Garvine (1974), and subsequently by Stronach (1977), Ingram (1981), Freeman (1982), Lewis (1984), and Luketina and Imberger (1987), among others. As a result of prior investigation of simpler versions of this model (see Garvine 1982, 1984, 1987; O'Donnell and Garvine 1983; O'Donnell 1988; henceforth referred to as the Garvine and O'Donnell series) it has become apparent that these fronts can have important consequences for flow in the plume itself. In this addition to the series, the numerical techniques developed by O'Donnell (1988) are employed to further investigate the unsteady and horizontally two-dimensional behavior of a small scale river plume with particular emphasis on the distribution, timing and influence of interfacial friction and mixing.

A brief survey of the existing observations of small scale plumes is presented in the next section and previous theoretical work is summarized in section 3. The mathematical formulation of the model is presented in section 4 and is followed in sections 5 and 6 by the presentation and discussion of the numerical solutions to two sets of numerical experiments. These calculations simulate the growth of a plume in steady and unsteady ambient crossflows with results that are interpreted to yield plausible explanations of the formation, evolution and mixings of natural river plumes. In section 7, the work presented is summarized and its implications discussed.

2. Observations

Using the data from a well-designed and executed series of observation campaigns, Garvine (1974, 1975, 1977) and Garvine and Monk (1974) characterized the flow field and hydrography at the mouth of the Connecticut River during periods of high discharge.

Corresponding author address: Dr. James O'Donnell, Department of Marine Sciences, University of Connecticut, Groton, CT 06340.

These studies still form the most complete river plume dataset available and motivated the model developed in this paper. In the spring, the fresh water discharge of the Connecticut River can be of the order of 2000 $m^3 s^{-1}$ and during these periods of high discharge, very low salinity water can be found in a shallow layer beyond the river mouth, in Long Island Sound itself. Figure 1 shows a map of the isohalines at 0.5 m on 21

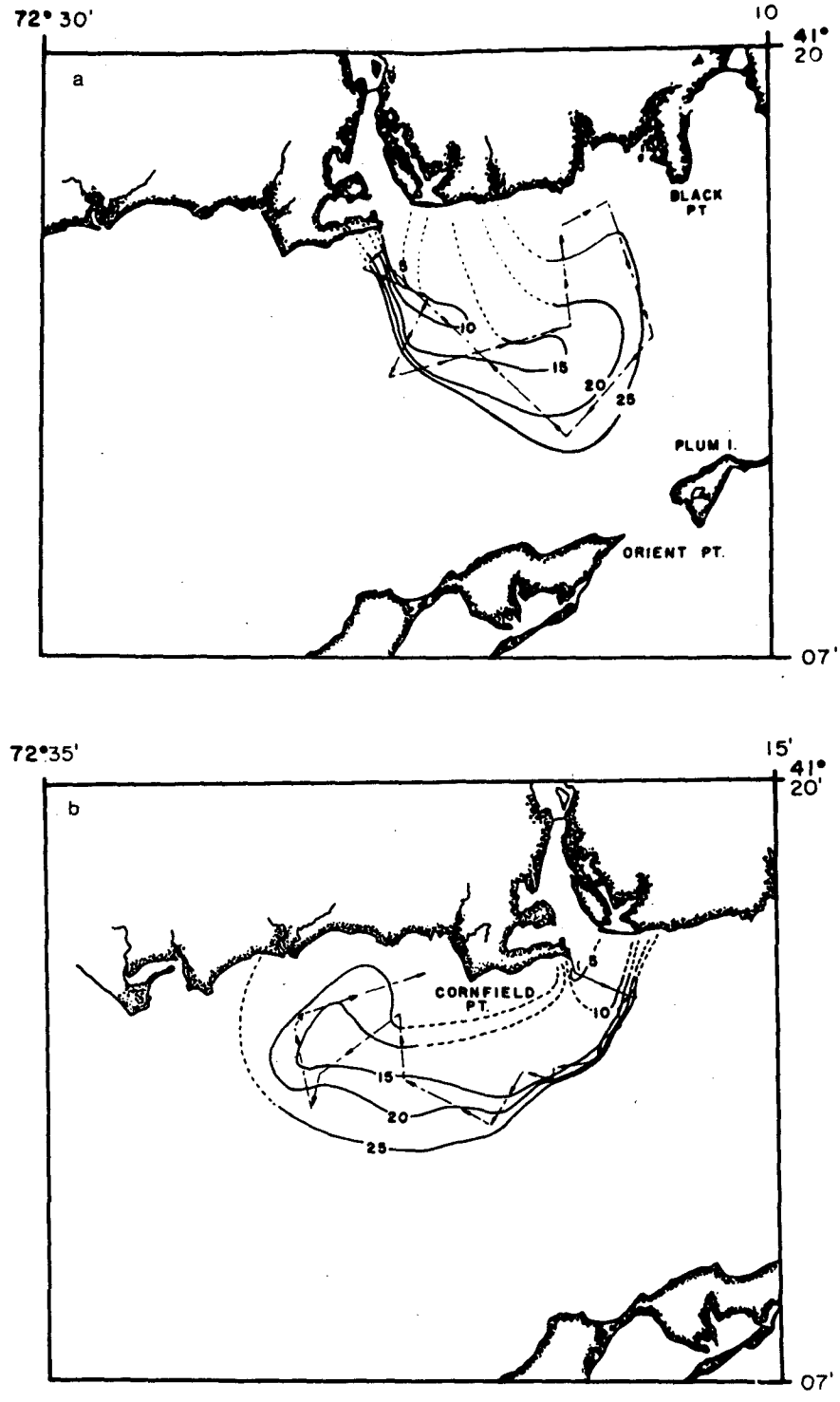

FIG. 1. The near surface salinity distribution at the mouth of the Connecticut River at approximately low slack water (a) and high slack water (b) on 21 April, 1972 From Garvine (1974).

April 1972. The extent of the freshened area is dramatic; 50 km^2. Figure 1a, shows the salinity field at low slack water, and it is apparent that the fresh water has been deflected to the east, presumably through an interaction with the ebbing tidal current. Figure 1b shows the salinity field at the end of the subsequent flood. Here the plume is to the west. The dynamics of the transition between these two states and the fraction of the plume volume that stays in the plume during the transition, a parameter of interest when considering the dilution of pollutants, will be subjects of discussion.

In both parts of Fig. 1 the isohalines tend to cluster on the upstream (with respect to the crossflow) side of the plume and indicate that a large spatial gradient in salinity exists. These regions often coincide with the position of a foam line and a discontinuity in water color that partially surrounds the plume layer. A photograph that clearly displays these features of the frontal region is presented by Garvine and Monk (1974), together with the results of observations of the hydrography and circulation in the neighborhood of the front. Figure 2, from their paper, is a representative cross section of density in the direction normal to the front and shows it to be a narrow region (of order 50 m) of strong mixing between the brackish plume water and that of Long Island Sound. A localized downwelling and consequent surface convergence of approximately 0.2 m s^{-1} was also reported. The disparity in the length scales of the plume and the front is an important aspect of plumes which is exploited in the model presented here, in the same way as in previous models in the Garvine and O'Donnell series.

The larger scale motion field was investigated by Garvine (1977) who employed drogues and drifters to estimate velocities in the plume and in the sound. Comparison of drogue tracks passing under the plume to those farther offshore showed that the water of Long Island Sound was not significantly influenced by the upper layer. This simplifies the modeling task since, if the upper layer is in isostatic equilibrium, the flow in the lower layer may be specified arbitrarily. Of course this is not an entirely satisfactory approximation since near the coast the layer depths are of similar magnitudes

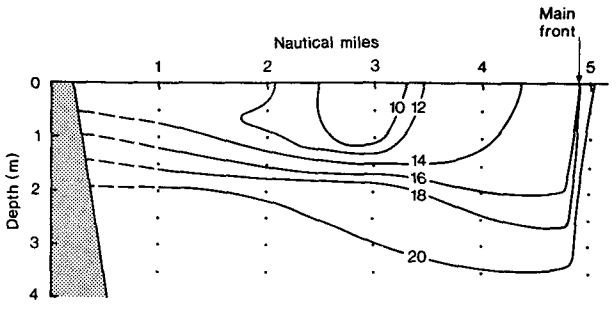

FIG. 2. An example density cross section along a line normal to the surface front in the plume of the Connecticut River. Density is expressed in σ_t units.

but, as it leads to a considerable simplification of the mathematical formulation, it is appropriate to study this simpler model first. In addition, the success of previous models that employ the isostatic approximation in describing some important features of the Connecticut River plume indicate that the nearshore effect of interactions between the layers is not extremely important.

There have been many other observations of river plumes. The Frazer River has been observed by Stronach (1977) to form a significant plume in the Strait of Georgia with strongly convergent fronts bounding a thin, highly stratified layer. Ingram (1981) described the outflow produced by the Great Whale River in Hudson Bay and, though measurements were difficult, also found that a frontally bounded plume structure occurred. Freeman (1982) studied the mixing of water from the La Grande River in James Bay during the ice covered season and observed that a highly stratified layer was present at the mouth of the river and, though strong fronts were not observed, this may have been due to the necessarily sparse sampling scheme. At the mouth of the Tees, however, Lewis (1984) reported a frontally bounded plume that formed on the ebb tide and described its behavior as similar to that of the Connecticut plume. More recently, unambiguous observations of a small scale, frontally bounded plume at the mouth of the Leschenault estuary have been reported by Luketina and Imberger (1987).

Larger scale plumes from major rivers and estuaries have also been documented. Bowman and Iverson (1977) and Mayer et al. (1979) found a highly variable plume at the mouth of the Hudson River and Boicourt (1973) traced the outflow of the Chesapeake Bay. Large plumes at the mouth of the Mississippi (Wright and Coleman 1971; Wiseman et al. 1975) and Yangtze rivers (Beardsley et al. 1985) have also been observed. The clarification of the steady state dynamics of these features was the subject of the recent model of Garvine (1987), and Chao and Boicourt (1986) have studied the time dependent behavior using a three dimensional, primitive equation model. Though there are features common to both large and small scale plumes, the dominant effects of the high frequency (tidal) variability in the ambient flow on the behavior of small scale plumes combined with the modest, second-order influence of the Coriolis effect causes small scale river plume dynamics to be significantly different from their larger scale counterparts.

3. Previous models

Several models of the steady flow at the mouth of an estuary driven by the brackish discharge have been applied to the plumes of large scale estuaries like the Delaware and Chesapeake bays (Beardsley and Hart 1978; Zhang et al. 1987). However these are clearly inapplicable to the highly time-dependent, small scale,

nonlinear plumes like that of the Connecticut River, which are the focus of this paper.

Stronach (1977) developed a time-dependent layer model of the circulation in the Strait of Georgia. The author was aware of the presence and potential importance of plume fronts and incorporated their effects by an unusual parameterization of mixing processes, which effectively caused strong gradients in the computed buoyancy of the upper layer. With the suitable selection of parameter values, predictions resembled the observed salinity field (Royer and Emery 1985), however the ad hoc nature of the assumptions restrict the general validity of the model and are unsuitable for an investigation of the fundamental dynamics of river plumes.

Freeman (1982) developed a model of the La Grande River plume using a similar conceptual framework to Stronach's, but simplified in that he solved for the steady, tidally averaged, state. This restriction allowed much more efficient computation of solutions and removed the need for artifices introduced by Stronach to mimic frontal dynamics, since the averaging effectively smears small scale fronts over a larger area.

Garvine (1982) presented a layer model of the plume produced by the steady discharge of buoyant fluid into a steady, ambient crossflow. In this model, the first in the Garvine and O'Donnell series, the effects of Coriolis acceleration, friction and mixing, were neglected and the discharge exited from a rectangular channel that intersected the coastline current at a variable angle and interacted with a steady flow in the ambient coastal water. This model exhibited several characteristics of observed plumes and explained the circumstances under which the plume separates from the shoreline. If the angle between the discharge and the coast exceeds a maximum determined by the flow variables at the discharge, the plume layer thickness will be zero at the coast on the downstream side of the discharge. Garvine also pointed out that this inshore edge would be subject to vertical mixing through shear instability.

Jones (1983) presented a similar, steady model for the flow from a radially symmetric discharge into a steady crossflow and found solutions which were in many respects similar to that of Garvine (1982). This geometry was further investigated by Garvine (1984) who solved the unsteady problem of the growth of a plume from a circular source in the absence of crossflow. These models predict plumes with the same basic radial structure. From the source, the layer thins towards the front but at approximately unit radius from the front, jumps to roughly the depth of the front. The flow field may therefore be described as a deep outer ring of unit width separated from the source by a very thin layer which, presumably, is susceptible to vertical mixing in the same way as the inshore edge of the plume in the two-dimensional, steady model of Garvine (1982). The interior jump in layer depth occurs where upstream propagating waves generated at the front are arrested by the accelerating flow from the source and coalesce. This tendency for the formation of large amplitude changes in flow properties over small spatial scales was also found to be an important aspect of the response of a plume to changes in the source discharge in the one-dimensional, unsteady model of O'Donnell and Garvine (1983).

The time-dependent growth of a plume from a steady, circular source has been studied by O'Donnell (1988). As the front propagates from the source, it is decelerated on the upstream side with respect to the crossflow, and the depth of the layer at the front increases. On the downstream side, the crossflow accelerates the front and decreases the depth of the plume layer. The influence of the crossflow on the front then propagates back into the plume creating an asymmetric analog of the interior jump found in Garvine's (1984) solution. When fluid passes through the jump into the deeper part of the layer, it experiences an alongfront pressure gradient, which tends to turn fluid offshore and alongshore in the direction of the ambient flow. Eventually, the region near the discharge reaches a locally steady state with the front far enough upstream that the layer-depth distribution along the front and the frontal position combine to set the pressure field to divert all of the effluent downstream. On the downstream side of the discharge of course, the plume continually expands and the layer thins until shear instability erodes and disperses the buoyant layer.

Obviously there are some significant differences between the flow from a straight channel considered by Garvine (1982, 1987) and the radially symmetric discharge of Jones (1983), Garvine (1984) and O'Donnell (1988). But, since these models all assume that a lower ambient layer exists that is much thicker than the plume, the question of which geometry is more characteristic of natural river plumes is moot; a real river mouths have complicated channel geometry and are often shallow. However, the success of these models in describing some of the important behavior of river plumes farther offshore prompts the consideration of dynamically more complicated and time-dependent problems, that are the subject of this paper, prior to the extension of the approach to problems, with two active layers, realistic geometry and bathymetry. The model summarized in the next section is the first unsteady, nonlinear layer model that allows asymmetry and employs physically reasonable frontal boundary conditions in a mathematically consistent manner.

4. The model

The model presented here is an extension and generalization of the models in the Garvine and O'Donnell series. The principal common feature of these models is the division of the plume into two dynamically distinct domains. The larger, the plume body, is idealized

as a vertically uniform layer with dynamics that, to lowest order, are inviscid and where mixing is strongly suppressed by the intense stratification. The second domain, the frontal zone, bounds the plume body, and separates it from the ambient fluid. The dynamics of this narrow boundary region are highly dissipative, with both friction and entrainment being important, as is the case in the Connecticut River plume front. The difference in length scales allows the frontal zone to be treated mathematically as a discontinuity at which integrated versions of the governing equations must be satisfied. This approach is basically the same as that applied to problems in compressible gas flow where the shock wave is the analog to the front in this problem.

The novel features of this model are: the plume is allowed to be two dimensional and time dependent; it may be of large enough scale that the Coriolis effect exerts some influence on the flow; interfacial mixing and friction are incorporated in the dynamics of the plume, though they must be small to be consistent with the assumed existence of a layer structure; the effect of a reversing crossflow is considered. It may be considered as the unsteady generalization of the models of Garvine (1982) and Jones (1983), or the extension of the unsteady models of O'Donnell and Garvine (1983) and Garvine (1984) to include the effects of nonzero crossflow, rotation, mixing and friction.

a. *The governing equations*

The model plume is a buoyant layer, of thickness D, thin compared to the total fluid depth. Within the plume, horizontal velocity components, u and v, and the buoyancy, b, are vertically uniform, though horizontally and temporally variable. The continuity principle for this regime may be stated as

$$\frac{\partial uD}{\partial x} + \frac{\partial vD}{\partial y} + \frac{\partial D}{\partial t} = q \tag{1}$$

where q is the rate of entrainment into ($q > 0$), or out of ($q < 0$), the layer. The layer buoyancy is defined, $b = g(\rho_a - \rho)/\rho_a$, where ρ_a is the density of the ambient fluid, and, since the fluid is incompressible, conservation of mass requires

$$\frac{\partial bD}{\partial t} + \frac{\partial buD}{\partial x} + \frac{\partial bvD}{\partial y} = qb_e - B_z. \tag{2}$$

Here, qb_e is the flux of buoyancy caused by entrainment. If the direction of entrainment is upward, then $b_e = 0$, and alternatively, if downwards $b_e = b$. The turbulent flux of buoyancy in the vertical direction, B_z, is towards the region of lower buoyancy, i.e. downward; B_z is therefore positive. The turbulent flux and the entrainment flux have been separated here, as they will be in the momentum equations, to emphasize that they arise from different mechanisms that may be competing. The entrainment term qb_e appears because the surface $z = -D(x, y)$ is not material, but one that may advance or retreat through the fluid.

The upper layer momentum equations are

$$\frac{\partial uD}{\partial t} + \frac{\partial u^2D}{\partial x} + \frac{\partial uvD}{\partial y} - fvD = -\frac{1}{2}\frac{\partial bD^2}{\partial x} + qu_e - F_x \tag{3}$$

$$\frac{\partial vD}{\partial t} + \frac{\partial uvD}{\partial x} + \frac{\partial v^2D}{\partial y} + fuD = -\frac{1}{2}\frac{\partial bD^2}{\partial y} + qv_e - F_y \tag{4}$$

where f is the Coriolis parameter, and F_x and F_y are the turbulent interfacial momentum fluxes in the x and y directions, respectively. The entrained velocities u_e and v_e are determined by the sign of q, as in the buoyancy equation:

$$u_e, v_e = \begin{cases} u_a, v_a: & q \geq 0 \\ u, v: & q < 0 \end{cases} \tag{5}$$

where u_a and v_a are the velocity components in the lower layer. The turbulent momentum fluxes are always directed towards the layer with the lower velocity component.

Surface fluxes of buoyancy and momentum are omitted from this formulation of the model to make plain the influence of the more predictable forcing mechanisms, but could be included with minimal effort. Also, a simple order of magnitude analysis that compares the acceleration of a buoyant layer by a moderate wind to the convective acceleration near the source of a small scale river plume indicates that the direct effect of the wind is of secondary importance to the evolution of a small plume in most circumstances. For example, a wind velocity of 10 m s^{-1} would produce a surface stress of roughly 0.1 Pa and result in the acceleration of a 1 m thick layer of fluid at 10^{-4} m s^{-2}. In contrast, the convective acceleration near the mouth of the a 1 km wide source is of order 10^{-3} m s^{-2}, a factor of 10 greater than that driven by the wind. In larger plumes, however, the local windstress is relatively more important since spatial derivatives are smaller.

b. *Parameterization of mixing and friction*

Though this model, and the others in the Garvine and O'Donnell series, assume rates of interfacial mixing and friction are small in the plume region, there are circumstances in which this is unrealistic. The radial discharge problem of Garvine (1984), for example, demonstrates a tendency to form ring structures that become separated from the discharge location by a region in which the layer depth tends to zero. As Garvine pointed out, this ultimately must result in mixing through the shear-flow instability process. Though the

nonlinear dynamics of the plume is the central focus of this investigation, interfacial transport is included because it does not complicate the task of solving the model equations, yet includes the possibility of the modification of the upper-layer horizontal pressure gradient by spatially inhomogeneous vertical mixing. Of course, vertical mixing has a dominant role in the ultimate mixing and dispersion of the plume water, circumstances in which a layer model loses meaning. It is shown subsequently, however, that the model is not overly sensitive to the magnitude of the parameters controlling the importance of vertical mixing.

Following Jones (1983), bulk formulae are employed to parameterize the interfacial transports:

$$q = E|\mathbf{u} - \mathbf{u}_a|,$$

$$B_z = C_f \sigma b|\mathbf{u} - \mathbf{u}_a|,$$

$$F_x = C_f(u - u_a)|\mathbf{u} - \mathbf{u}_a|,$$

$$F_y = C_f(v - v_a)|\mathbf{u} - \mathbf{u}_a|. \qquad (6)$$

The friction coefficient, $C_f = O(10^{-3})$, and the turbulent Prandtl number, $\sigma = O(1)$, are assumed to be constants, but it is well established, see Turner (1973), that the entrainment coefficient E is proportional to the local Richardson number, defined here as $\mathrm{Ri} = c^2/|\mathbf{u} - \mathbf{u}_a|^2$. Jones (1983) compared the various formulations of the functional relationship $E(\mathrm{Ri})$ that have been developed by Jirka (1982), Stolzenbach and Harleman (1971), and Koh and Fan (1970), to the measurements of Ellison and Turner (1959) and showed that they all adequately described the data. The Stolzenbach and Harleman (1971) expression is employed here and formulated in terms of the bulk shear Froude number, $F_\Delta = |\mathbf{u} - \mathbf{u}_a|/c$ or equivalently $\mathrm{Ri}^{-1/2}$, and may be written as

$$E = E_1 e^{5(1-F_\Delta^{-1/2})}. \qquad (7)$$

The constant $E_1 = 0.6 \times 10^{-5}$ is the entrainment coefficient for $F_\Delta = 1$.

The neglect of wind induced mixing across the interface of the plume, implicit in the parameterization of mixing rate, is justifiable since it is small compared to that typically produced by the large shear across the interface.

c. *Coordinate system and boundary conditions*

The coordinate system employed is sketched in Fig. 3. The origin is at the center of the discharge channel with the y-axis along the coast and the x-axis offshore. The buoyant layer is forced by a specified radial transport from a semicircular boundary of radius $L_c/2$, where L_c is the width of the discharge channel. A radially symmetric discharge is imposed to avoid some computational difficulties which are discussed by O'Donnell (1988). On the boundary ($x = 0$, away from the source, the condition of no flow normal to the coast

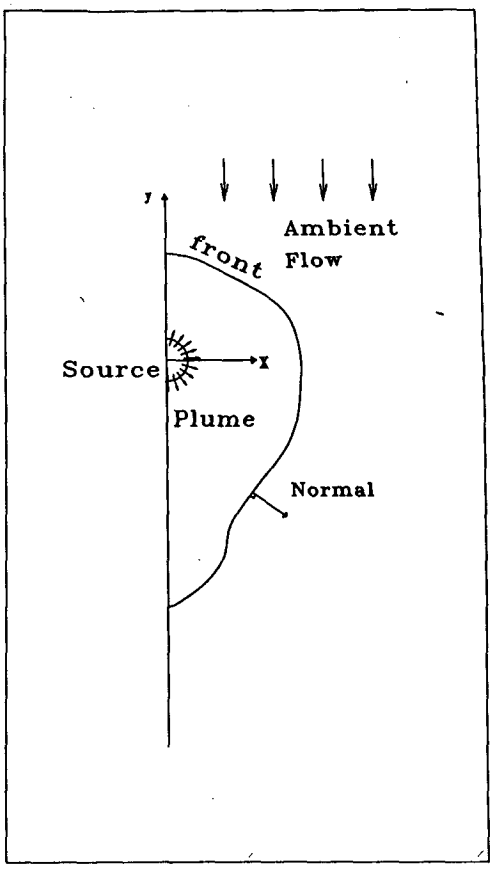

FIG. 3. The coordinate system and source-boundary geometry.

is enforced ($u = 0$). At the source, since the speed of the discharged fluid, q_{in}, is greater than or equal to the local phase speed, $c_{\mathrm{in}} = (b_{\mathrm{in}} D_{\mathrm{in}})^{1/2}$, all variables must be specified.

At the front, the assumption that the length scale of the front is much smaller than that of the plume is exploited and the conditions of Garvine (1981) are imposed. The notation D_0, b_0 and $\mathbf{u}_0$ is adopted to denote the limiting values of the layer depth, buoyancy, and velocity in the plume when approaching the dissipative region, and $\mathbf{u}_a$ is the local ambient flow velocity. Figure 3 indicates that the front moves in the direction $\mathbf{n}$, the local normal, at a velocity u_f relative to a fixed origin. By assuming that the frontal dynamics is steady (in a frame moving with the front) and adopting an ad hoc parameterization of the entrainment and friction, the following jump conditions may be derived:

$$u_f - \mathbf{n} \cdot \mathbf{u}_a = c_0 F \qquad (8a)$$

$$u_f - \mathbf{n} \cdot \mathbf{u}_0 = A(u_f - \mathbf{u} \cdot \mathbf{u}_a) \qquad (8b)$$

where the phase speed c_0 is defined as $c_0 = (b_0 D_0)^{1/2}$. Relation (8a) may also be regarded as an expression of the experimental observation that the front of a gravity current spreads relative to the ambient water

at a speed proportional to the phase speed just behind the front, cf. Britter and Simpson (1978) and Sargent (1983), with a frontal Froude number, F, close to unity. The second condition, (8b), states that the convergence at the front is proportional to the bulk shear between the plume and the ambient water at the front. The constant of proportionality, A, is inadequately measured but is certainly small.

Using the width of the discharge and the values of the variables there as scales, new dimensionless variables may be defined as $D^* = D/D_{in}$; $u^* = u/c_{in}$; $v^* = v/c_{in}$; $b^* = b/b_{in}$; $x^* = x/L_c$; $y^* = y/L_c$; and $t^* = tc_{in}/L_c$; then, when these are substituted in the governing equations (1)–(4) containing the bulk mixing and friction formulae (6), we find that the new system contains four dimensionless parameters; $R_E = E_1 L_c \times D_{in}$, the scale for entrainment effects; $R_F = C_f L_c / D_{in}$, the scale for frictional effects; $R_K = fL_c/c_{in}$, the Kelvin number reflecting the importance of the Coriolis effect to the dynamics, and σ, a Prandtl number describing the relative effectiveness of interfacial turbulence in transporting buoyancy and momentum between the layers. The governing equations are now,

$$\frac{\partial D}{\partial t} + \frac{\partial uD}{\partial x} + \frac{\partial vD}{\partial y} = R_E|\mathbf{u} - \mathbf{u}_a| \tag{9}$$

$$\frac{\partial bD}{\partial t} + \frac{\partial buD}{\partial x} + \frac{\partial bvD}{\partial y} = \{R_E b_e - R_F \sigma b\}|\mathbf{u} - \mathbf{u}_a| \tag{10}$$

$$\frac{\partial uD}{\partial t} + \frac{\partial u^2 D}{\partial x} + \frac{\partial uvD}{\partial y} + \frac{1}{2}\frac{\partial bD^2}{\partial x} = R_K vD + \{R_E u_e + R_F(u_a - u)\}|\mathbf{u} - \mathbf{u}_a| \tag{11}$$

$$\frac{\partial vD}{\partial t} + \frac{\partial uvD}{\partial x} + \frac{\partial v^2 D}{\partial y} + \frac{1}{2}\frac{\partial bD^2}{\partial y} = -R_K uD + \{R_E v_e + R_F(v_a - v)\}|\mathbf{u} - \mathbf{u}_a|. \tag{12}$$

The asterisks are omitted here and subsequently to simplify the notation, and all variables are henceforth dimensionless.

d. The method of solution

The solution of this system of partial differential equations and boundary conditions is classified mathematically as a quasi-linear hyperbolic free boundary value problem, and is rather difficult to solve. A numerical scheme, which yields approximate solutions, is described and demonstrated in some detail by O'Donnell (1986, 1988) and is employed here to study the unsteady dynamics of river plumes. The method employs a novel mixture of a finite difference scheme in the plume and the method of bicharacteristics to obtain the solution at the front. It is fundamentally the two-dimensional generalization of the scheme employed by O'Donnell and Garvine (1983).

5. The formation of a river plume

The growth and adjustment of a model river plume in a steady crossflow was described recently by O'Donnell (1988) and summarized in the previous section. Here, the sensitivity of those calculations to various model parameters is explored in more detail to determine: 1) the evolution and structure of plumes which encounter crossflow velocities in the range $-1.5 \leq v_a \leq -0.5$, 2) the influence of the acknowledged uncertainty in the frontal parameters on the adjustment process and on the final state, 3) the role of the Coriolis effect, and 4) the consequences of interfacial mixing and friction. These calculations also allow the assessment of synergistic interactions among the various mechanisms incorporated in the model.

In the numerical experiments discussed in this and the following sections, the layer depth and the buoyancy at the source were unity, and the radial transport was $2^{1/2}$. Simple and convenient initial conditions were employed which specified that the plume started as a stationary ring of unit radius surrounding the discharge and calculations were performed using the numerical scheme of O'Donnell (1988) with a grid size, $\Delta x = 0.1$, Courant number, $C_N = 0.7$ and artificial viscosity parameter $\nu = 0.2$.

a. The crossflow velocity

The influence of the magnitude of the crossflow velocity on river plume evolution is illustrated in the results of experiments 1, 2 and 3, in which $v_a = -1.5$, $v_a = -1.0$, and $v_a = -0.5$ are presented in Figs. 4 and 5. In these calculations, rotation, mixing and friction in the interior of the plume were absent ($R_K = R_F = R_E = 0.0$) and the frontal parameters were chosen for simplicity as $A = 0$ and $F = 1$. Figures 4a–c show contour plots of the buoyant layer thickness, the frontal position and transport vectors at $t = 7.0$ in experiments 1, 2 and 3. The solution with $v_a = -1.0$, Fig. 4b, displays the same general structure found by O'Donnell (1988) and the effect of the stronger crossflow can be assessed by comparing it with Fig. 4a. The evolution and the general shape of the plume, as defined by the frontal position, is only slightly modified by the magnitude of the crossflow. The stronger ambient flows cause more rapid spreading in the downstream direction but curtail the frontal propagation upstream and offshore, resulting in a slight reduction in the curvature of the front on the upstream side of the plume. The total area enclosed by the front is only weakly affected however, and the differences in the solutions are most clearly marked by the distribution of the interface depth or plume thickness. In Fig. 4a, the flow throughout most of the plume is smooth with high gradients restricted to the small region on the upstream side of the plume between the source and the front. This is only marginally resolved by the calculation. Smaller crossflows, see Fig. 4c, allow more spreading and the consequent formation of an interior jump in layer depth which has

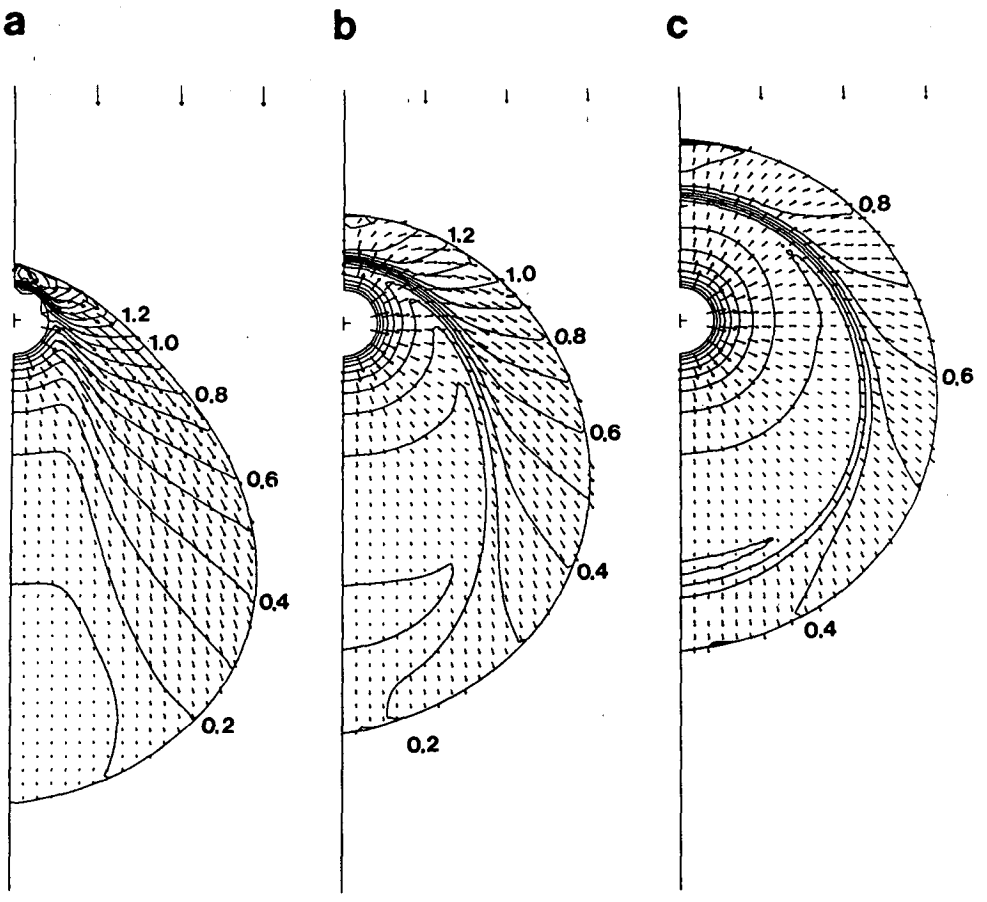

FIG. 4. Contours of layer depth, the frontal position, and transport vectors at $t = 7.0$ in experiments 1–3, with crossflow velocities of (a) $v_a = -1.5$, (b) $v_a = -1.0$, (c) $v_a = -0.5$.

an amplitude that appears to be inversely proportional to the magnitude of the crossflow. The flow structure is then basically the same as that described by Garvine (1984) but with the flow in the deep outer "ring" modified by the crossflow. When the front is trapped near the source by larger crossflow velocities, the formation of an interior jump is inhibited and a flow more like that described by the Garvine (1982) results.

Since mixing and dispersion of river water in the coastal ocean is of considerable importance, the possibility of vertical interlayer transport must be considered. The areas in which mixing driven by Kelvin-Helmholtz instability at the interface is likely can be identified simply, as was pointed out by Garvine (1982), by examining the distribution of the bulk shear Froude number, F_Δ. Vigorous mixing should be expected for $F_\Delta > 2$ (equivalent to the Richardson number, Ri $< \frac{1}{4}$). Contours of F_Δ are presented in Fig. 5 for experiments 1 to 3 and the areas in which $F_\Delta < 2$ are shaded. It is clear that smaller crossflow velocities result in larger areas of high F_Δ and, presumably, vigorous vertical mixing. There is a simple explanation for this rather unexpected result. Shear instability is likely in areas where the layer has thinned and accelerated as a result of buoyant spreading and where there is a significant component of the flow velocity in the plume in a different direction to that of the ambient flow. Larger crossflow velocities have been shown to curtail spreading in the upstream direction with the result that thin areas of the plume only occur on the downstream side of the discharge where both the ambient and buoyant fluid move in the same direction.

If interlayer transport was explicitly included in the model, then the adjustment and equilibrium state of the plume could be drastically modified. Therefore, calculations incorporating these effects will be presented and discussed after the influence of the frontal parameters and rotation on the simpler inviscid and immiscible model are examined.

b. Sensitivity to the choice of frontal parameters

The sensitivity of the behavior of the plume to the selection of values of the frontal parameters A and F must also be considered here since there remains some uncertainty about the choice that best represent the friction and exchange mechanisms in natural river plumes. Field observations by Garvine and Monk (1974), the laboratory experiments of Britter and

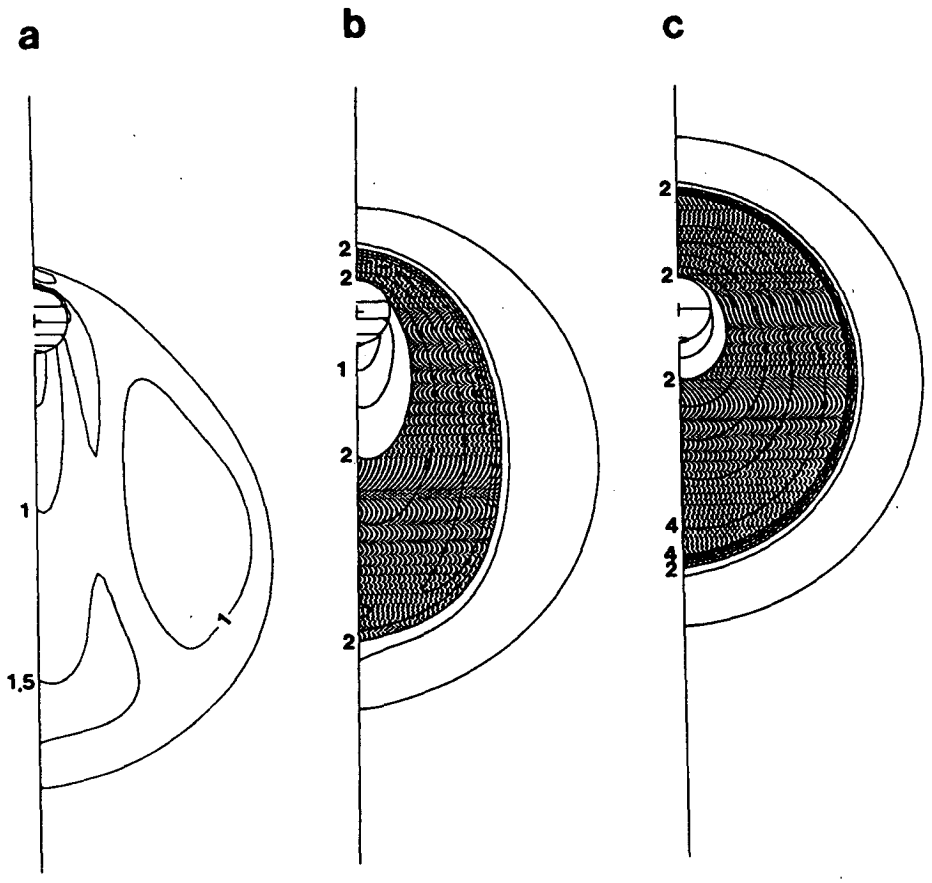

FIG. 5. Contours of F_Δ, the bulk shear Froude number, and the frontal position at $t = 7.0$ in experiments 1–3. Regions in which $F_\Delta \geq 2$ have been shaded.

Simpson (1978) and the theoretical work of Benjamin (1968) agree that the Froude number F lies in the range $1 \leq F \leq 2^{1/2}$ and that $-0.2 \leq A \leq 0.0$. Garvine (1982) investigated the influence of a variety of combinations of values for A and F on his steady model of river plumes. The experiments discussed subsequently illustrate the consequences of the parameter values in this unsteady model, but the results are consistent with his conclusions.

The influence of the choice of the frontal parameters on the solution obtained in experiment 2 demonstrates the important role of the frontal processes. Figure 6a presents the computed solution for the layer depth and transport vectors for experiment 2 at $t = 7.0$, in which $v_a = -1$, $F = 1$, and $A = 0$ (the same solution shown in Fig. 4c). This is to be compared to the results of experiments 4 and 5 (shown in Figs. 6b,c) in which the crossflow velocity was also $v_a = -1$, but $F = 2^{1/2}$ and $A = 0$, and $F = 2^{1/2}$ and $A = -0.2$, respectively. These values bound the estimated range of the parameters.

Large values of F require the front to move faster relative to the ambient flow, see (8a), allowing more buoyant spreading, which results in a larger plume and a more extensive area of radial flow near the source, as is evident in Fig. 6c. The net effect of increasing F is therefore similar to reducing the crossflow velocity but leads to less asymmetry in the maximum upstream and downstream propagation of the front. The influence of frontal entrainment out of the plume is demonstrated by experiment 5. As expected, there is less buoyant fluid in the plume since the deep region between the interior jump and the front is much narrower in Fig. 6c than in 6b. However, the area of the plume is almost the same. The direct effect of frontal entrainment then is to generate a frontal convergence that slows the propagation, into the plume, of waves generated at the front, causing the jump to form much closer to the front. This results in a greater area of radial expansion that, as has been demonstrated, is susceptible to vertical mixing. Clearly, although the direct effect of the frontal boundary conditions is local, their influence on the area and internal structure of the plume is significant. Therefore, F and A must be more accurately determined by field or laboratory observations.

c. *The effect of rotation*

The dimensionless form of the governing equations, (9) to (12), shows that the importance of the Coriolis

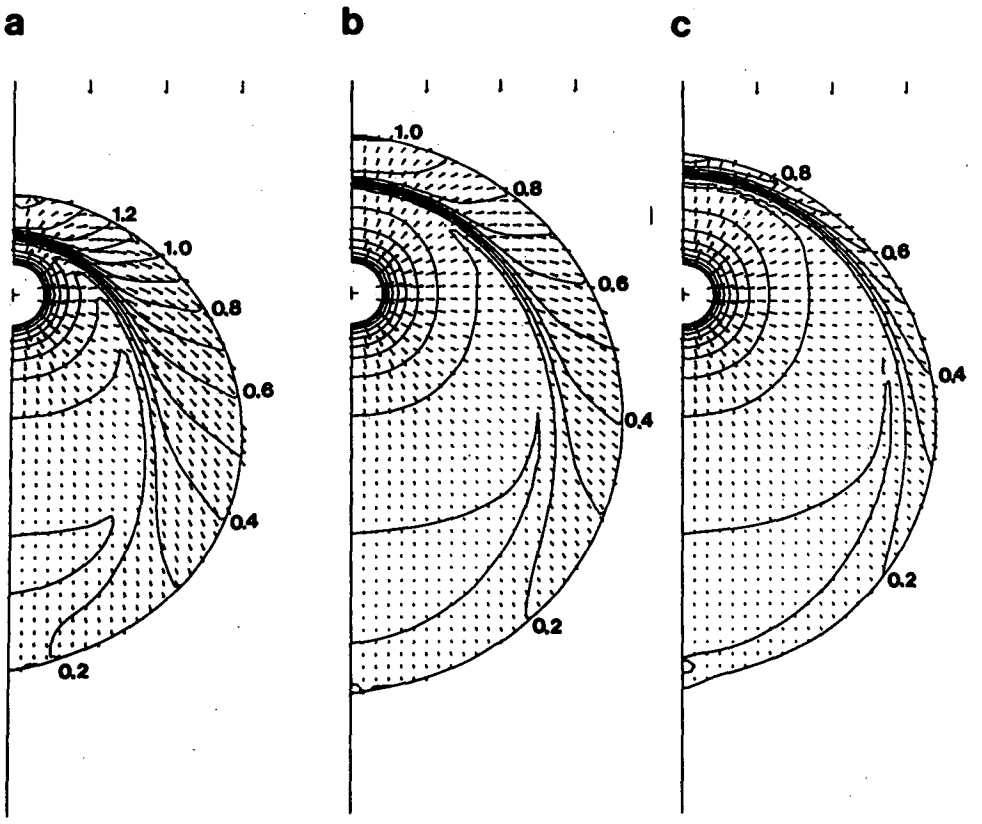

FIG. 6. Controus of layer depth, the frontal position and transport vectors at $t = 7.0$ in experiments 2, 4 and 5, with crossflow velocity $v_a = -1$ and frontal parameters (a) $F = 1$, $A = 0$, (b) $F = 2^{1/2}$, $A = 0$, and (c) $F = 2^{1/2}$, $A = -0.2$.

effect in the dynamics of a buoyant layer scales with the Kelvin number, R_K, the ratio of the geometric length scale to the internal Rossby radius of deformation. River plumes exhibit a wide range of values of this parameter. A reasonable estimate for the plume of the Connecticut River is $R_K = 0.2$, indicating that the Coriolis effect is relatively small. Nevertheless, it can subtly effect the evolution and erosion of the buoyant layer.

In the absence of the Coriolis effect the direction of the crossflow in the preceding experiments is immaterial. Had $v_a = 1$ been chosen, the resulting solutions would simply be the reflection of those shown about a line through the center of the discharge. Rotation breaks this symmetry. For positive values of R_K the buoyant fluid is deflected to the right of its direction of motion, thus opposing the influence of a positive alongshore flow, and conversely, in concert with a negative alongshore flow. This interesting cooperation and competition is quantitatively investigated by the comparison of the results of experiments in which $v_a = -1$, $F = 1$, and $A = 0$, but where with $R_K = 0.2$ (experiment 6), and $R_K = -0.2$ (experiment 7). Note that it is the sign of the Coriolis acceleration which is changed here rather than the direction of the crossflow. These are equivalent, however, this choice facilitates comparison.

Figures 7a–d show the evolution of the computed transport vectors and contours of layer depth for experiment 6 in which the Coriolis acceleration acts in concert with the ambient velocity. Comparison of this with Figs. 8a,b shows the consequences of competition. Differences between the solutions are manifest early in the formation of the plume and are most apparent just behind the front on the downstream side of the domain. The most dramatic contrast is in the layer thickness, and the offshore gradient in layer depth, along the coastal boundary. Positive rotation results in a small onshore transport that overcomes the tendency of the layer to shoal at the coast due to the expansion of the front (see Figs. 6a) and instead, causes the depth to increase and a significant boundary current to form at a distance R_K^{-1} to the right of the source and at approximately $t = R_K^{-1}$ (Figs. 7d). Negative rotation, on the other hand, enhances the shoaling tendency by inducing an offshore transport. Eventually, at approximately $t = R_K^{-1}$, the layer thins to zero causing the computation to be terminated.

The distribution of the bulk shear Froude number, Figs. 7e–h and 8c,d, suggests that the potential for shear instability develops as in the nonrotating solutions presented in Fig. 6, and that the influence of the Coriolis effect when acting in concert with the crossflow is to

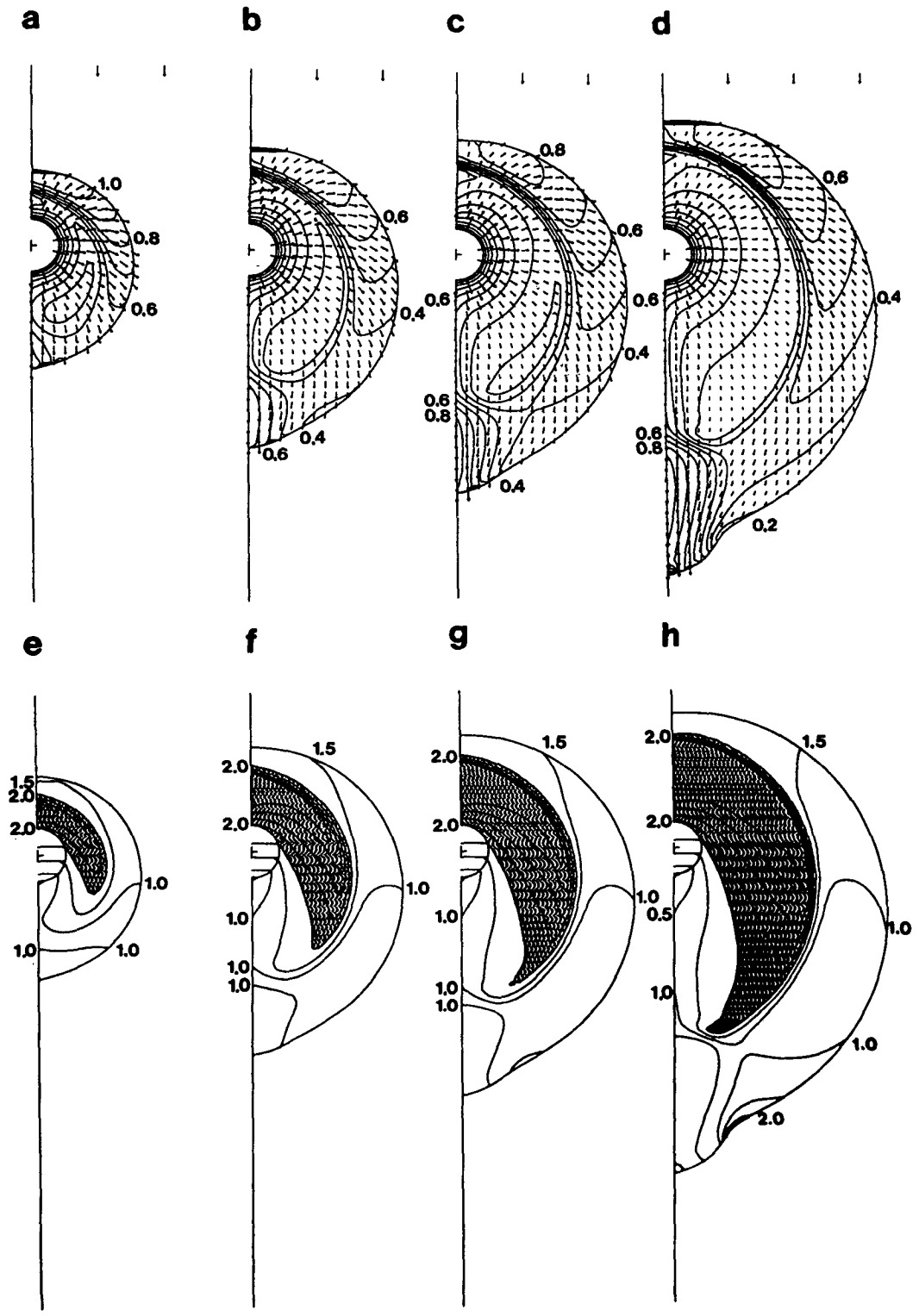

FIG. 7. The evolution of the solution in experiment 6 with crossflow velocity $v_a = -1$, frontal parameters $F = 1.0$ and $A = 0.0$, and Kelvin number $R_K = 0.2$. Figures 7a–d show contours of layer depth, the frontal position and transport vectors at $t = 2.37$, 4.63, 5.77, and 8.0 respectively. Figures 7e–h show the corresponding distribution of the bulk shear Froude number F_Δ with areas in which $F_\Delta \geq 2$ shaded.

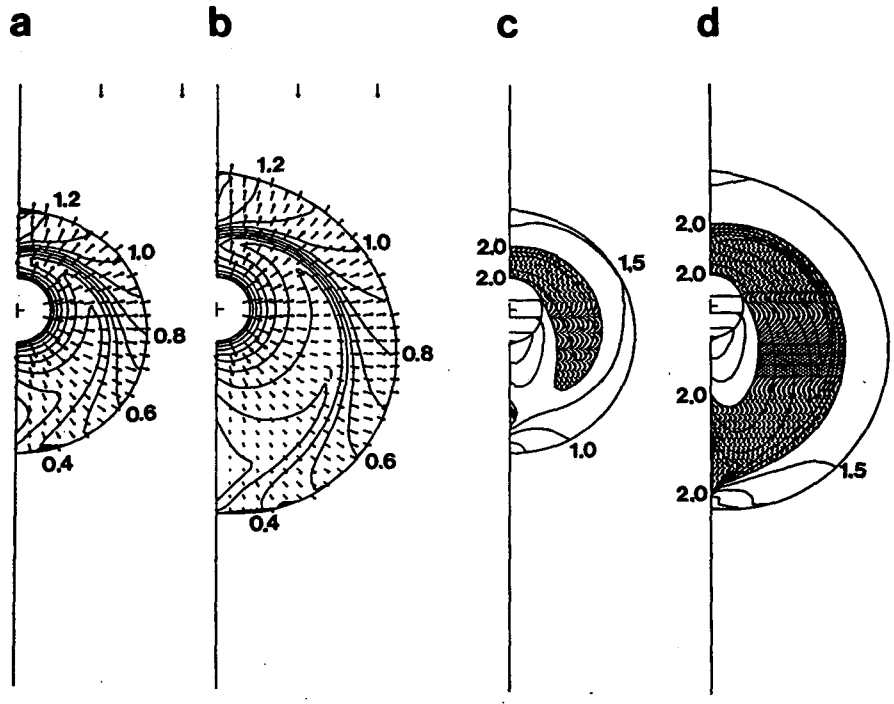

FIG. 8. The evolution of the solution in experiment 7 with crossflow velocity $v_a = -1$, frontal parameters $F = 1.0$ and $A = 0.0$, and Kelvin number $R_K = -0.2$. Figures 8a,b show contours of layer depth, the frontal positon and transport vectors at $t = 2.43$, and 4.26 respectively. Figures 8c,d show the corresponding distribution of the bulk shear Froude number F_Δ with areas in which $F_\Delta \geq 2$ shaded.

maintain lower values of F_Δ nearshore in the region of the boundary current formation. Competition, on the other hand, exacerbates the rate of shoaling of the interface resulting in enhanced mixing nearshore. This process may be of significance in the plume of the Connecticut River since the predominant circulation in the ambient water, Long Island Sound, is tidal and reverses every six hours. Indeed, the surface salinity maps of Garvine (1974), presented in Fig. 1, show a strong asymmetry, consistent with the interpretation that the nearshore side of the plume is more sensitive to vertical mixing when the direction of the crossflow is counter to that of the propagation of a free Kelvin wave.

d. The consequences of explicit mixing and friction

Some of the effects of vertical mixing are incorporated in this model (see section b) so that limitations of previous layer models may now be assessed. The assumption that in the presence of vertical mixing, the plume still behaves as a layer requires that the vertical structure of the component of the horizontal pressure gradient produced by spatially heterogeneous vertical mixing is unimportant. This ad-hoc simplification is rather unsatisfying but is consistent with the neglect of vertical variations in the magnitude of other terms in the horizontal momentum balances common to all long-wave models. Here we take the view that having a crude representation of the influence of mixing in the model is superior to having none. The results of the calculations presented in this section show that the net effect of mixing on the distribution of the interface depth can be quite significant.

The results of three numerical experiments, 8–10, in which both mixing and friction were active are presented in Figs. 9 and 10. Figure 9 shows the calculated distribution of layer depth, frontal position and transport vectors at $t = 7.0$ for ambient velocities of (a) -1.25, (b) -1.0, and (c) -0.5. Mixing parameter values $R_F = R_E = 0.1$ with a turbulent Prandtl number of $\sigma = 1$ and a frontal entrainment parameter of $A = -0.1$ were adopted since they are representative estimates for the plume of the Connecticut River. Other experiments with $R_F = 0$ showed similar results indicating that when mixing is allowed, its effects are much more significant than those of frictional processes.

Differences between these calculations and the results of experiments 1–3, see Figs. 4a–c, are principally due to the incorporation of the interfacial mixing mechanisms. Note, however, that the crossflow velocities employed in experiment 8 was slightly less than in experiment 1. This was necessary to ensure that the frontal boundary and the source boundary remain distinct.

At high crossflow velocities the distribution of layer depth in the plume does not appear to be strongly affected by entrainment (compare Figs. 4a and 9a). Of

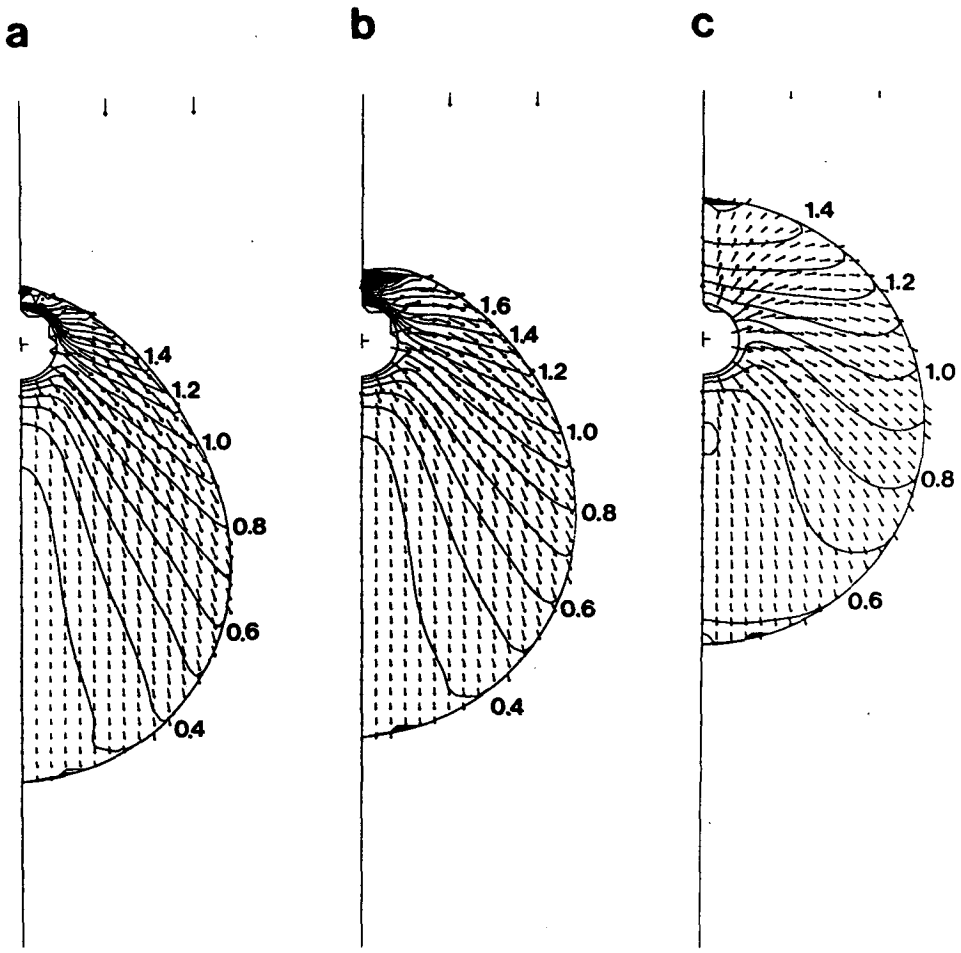

FIG. 9. Contours of layer depth, the frontal position and transport vectors at $t = 7.0$ in experiments 8, 9 and 10, with frontal parameters $F = 1.0$, and $A = -0.1$, Kelvin number $R_K = 0.0$, and entrainment and friction coefficients $R_E = R_F = 0.1$. The crossflow velocities were $v_a = -1.25$, -1.0, and -0.5, respectively.

course the plume is slightly deeper because of the entrainment of the lower fluid, and arealy smaller due to frontal entrainment out of the plume, but the general trends are similar. At lower crossflow velocities the structures are quite different. The vertical flux of mass and momentum from the lower layer destroys the radial symmetry and interior jump in layer depth that arises from the geometry of the discharge at low crossflow velocities (for example, compare Figs. 4e and 9d). The conclusion then is that the plume structure predicted in the absence of interfacial mixing, experiments 1 to 7, is unlikely to exist in a natural river plume since vertical entrainment limits shoaling of the interface. In addition, local interaction of the plume and the ambient flow "short-circuits" the ambient flow-front interaction responsible for the formation of the interior jump, the dominant feature of the immiscible plume structure.

The computed buoyancy distributions in experiments 8–10 are shown in Fig. 10. It is impossible to compare these results to field observations at the moment; however, Huq (1983) performed carefully controlled laboratory tank experiments which may be qualitatively compared to the calculations, and Fig. 11 shows an example distribution of buoyancy. The pattern of the contours is encouragingly similar to those of Fig. 10, particularly in the asymmetry of the buoyancy gradients on either side of the source. A quantitative comparison is complicated by the difficulty in translating Huq's source conditions to those used in this model and is therefore not presented here.

The results of experiments 6 and 7 suggested that the distribution of vertical mixing in the plume was sensitive to the relative directions of the crossflow and a free Kelvin wave. Experiments 11 and 12 further investigate this conjecture. In these experiments both friction and entrainment in the interior of the plume were allowed, with $R_E = R_F = 0.1$, and the frontal parameter values, $F = 1$ and $A = -0.1$ were employed. In both experiments, the ambient crossflow velocity was taken to be $v_a = -0.5$ to act in concert with the Coriolis effect to inhibit nearshore mixing in experi-

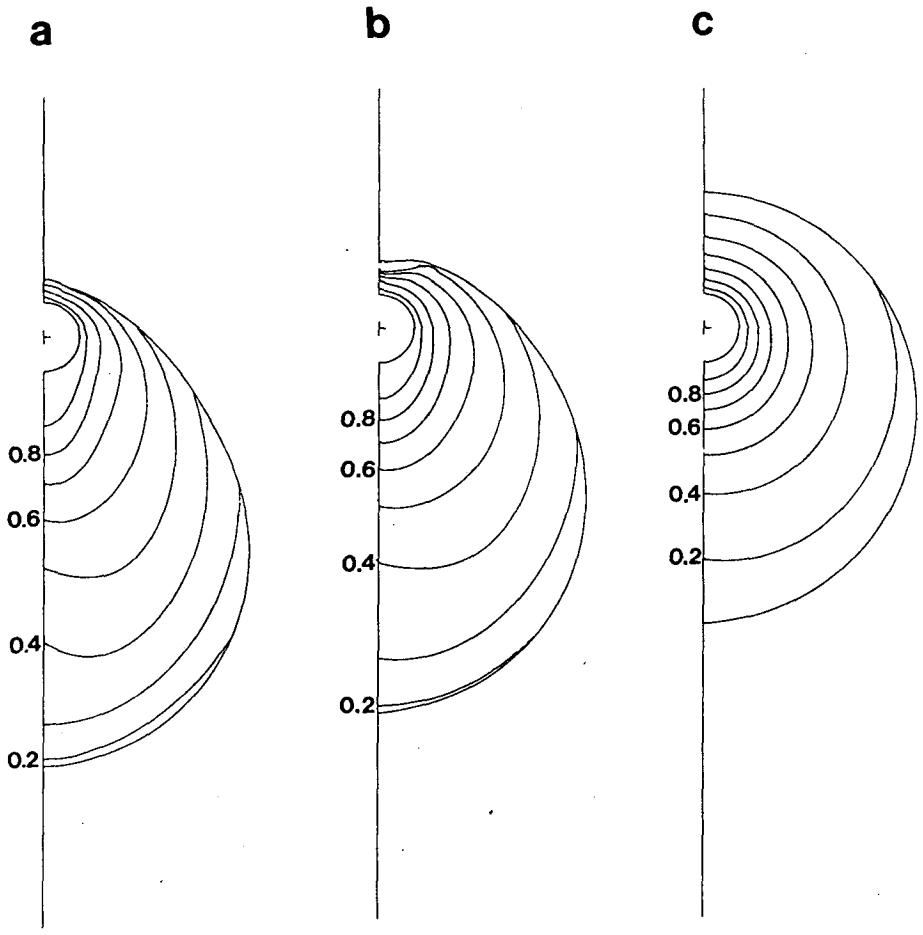

FIG. 10. Contours of buoyancy and the frontal position at $t = 7.0$ in experiments 8, 9 and 10, corresponding to the solutions shown in Fig. 9.

ment 11 ($R_K = -0.2$), and to compete with the Coriolis effect in experiment 12 ($R_K = -0.2$). Figure 12a shows the solutions for layer depth, transport, and frontal position at $t = 5.9$ from experiment 11 and Fig. 12b shows the corresponding distribution of the upper layer buoyancy. The equivalent solutions for experiment 12 appear in Figs. 12c,d.

Though the frontal positions in these experiments are similar, the effects of rotation are exhibited in the obvious differences between the solutions in the interior. In particular, the radial pattern of the transport vectors on the upstream side of the plume in Fig. 12c, contrasts with that in Fig. 12a where they are directed offshore and alongfront. The radial pattern is a result of an interesting balance between the pressure gradient imposed by the front–crossflow interaction and the Coriolis effect, and also indicates that the front has not reached its equilibrium position.

The layer depth distributions are also quite different from each other though they appear to have a structure similar to those obtained in the absence of mixing and friction, but it is interesting to note that the buoyancy distribution is only noticeably different nearshore on the downstream side of the plume. These results suggest that the effects of rotation on plumes from relatively narrow rivers like the Connecticut are most likely to be manifest in the distribution of the interface depth.

6. The fate of a river plume

In natural circumstances, river plumes experience fluctuations in the ambient flow velocity and often reversal of its direction, but to date, observations have not been able to describe how plumes respond to these variations. For example, it is clear from Garvine's (1974) observations (see Fig. 1) that during half of a tidal cycle the plume of the Connecticut River somehow moves from the east to the west side of the river mouth, but how does this occur? Available information is insufficient to determine either the fate of the brackish fluid or the main mechanisms of dispersion.

Two experiments to investigate this transition are discussed here. In the first, the change is abrupt; it essentially instantaneous compared to the time for the establishment of the plume. This experiment is a simple model of the modification of small scale plumes by

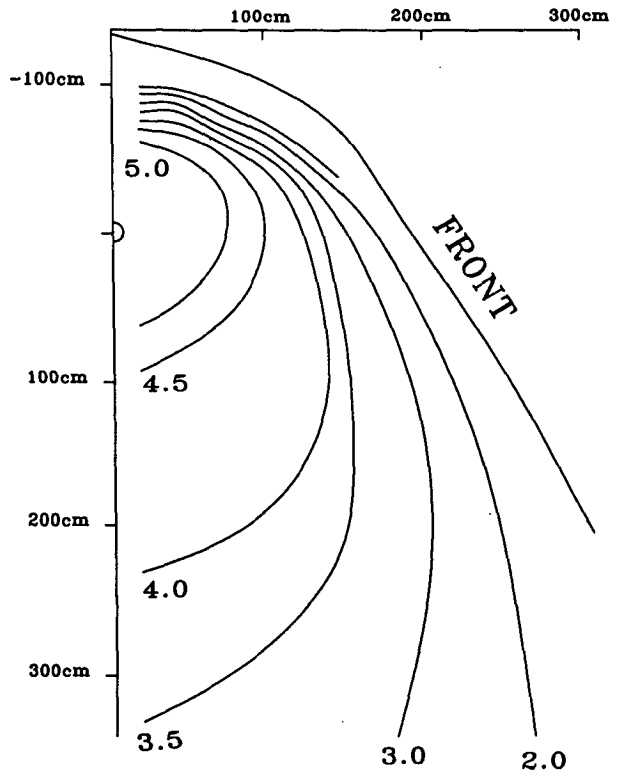

FIG. 11. Distribution of surface buoyancy in a laboratory experiment of Huq (1983).

wind driven ambient currents but also clearly demonstrates the essential character of the adjustment mechanisms. In the second experiment, the time scale of the ambient flow fluctuation is comparable to that of the plume formation, as in the case of the Connecticut River plume modulated by the tidally driven water of Long Island Sound. After the results of the experiments are described and interpreted, the implications of explicit mixing and rotation on the transition will be discussed.

a. The sudden reversal of the crossflow

The response of layer thickness of a plume to an abruptly reversed ambient crossflow is demonstrated in the computed solution to experiment 13, which is displayed in Fig. 13. Interfacial friction and mixing were omitted in this experiment, i.e. $R_E = R_F = 0$, and the frontal parameters values of $F = 1$ and $A = 0$ were employed. A small amount of rotation was included $R_K = 0.1$ to delay onset of the surfacing of the interface and the ambient flow velocity was specified to be $v_a = -1$ for $t \leq 8.0$, and $v_a = 1$ subsequently.

Thus, for $t \leq 8$, the solution is similar to that of experiment 2 and 7 (see Figs. 4 and 7). Figure 13a shows a projection of a three dimensional plot of the layer thickness as a function of x and y at $t = 7.8$, just before the ambient flow reversal. The consequences of the change are most readily appreciated by comparing Figs. 13a with 13b,c which show similar projections at $t = 8.7$ and $t = 10.6$, respectively.

Prior to the change in crossflow, the usual layer thickness distribution is exhibited. Notice in particular, the large value of the layer depth on the upstream side of the plume, the alongfront pressure gradient, the shoaling downstream region and the coastal current. Figure 13b shows the structure just after reversal of the crossflow, though from a slightly different viewpoint. The differences are dramatic. Since the front in the coastal current region now experiences a counterflowing ambient velocity, the frontal jump conditions require the depth to increase and the frontal velocity to reduce. This is propagated slowly into the plume as an internal surge; compare 13b and 13c.

Equally dramatic is the shoaling on what was previously the deep side of the plume. When the crossflow is reversed, the front is suddenly required to spread rapidly but, since the fluid behind must be accelerated, the depth at the front reduces sharply generating a rarefaction, or expansion wave, that propagates into the plume. Both the surge and the rarefaction can be seen in Fig. 13c, the solution at $t = 10.6$.

Calculation of the bulk shear Froude number distribution after the reversal establishes that most of the plume is subject to intense mixing when the crossflow is reversed because the shallow layer is suddenly subjected to much larger shear. During early stages of the spreading, the interaction of the crossflow with the front causes the buoyant fluid to be turned towards the downstream direction thus minimizing shear as was explained by O'Donnell (1988). But, when the crossflow is reversed, the interior of the plume is unaffected, in the absence of friction or mixing, until pressure disturbances generated at the front propagate to any particular location in the interior. Since little adjustment to the new ambient flow conditions can take place before vertical mixing becomes active, it is tentatively concluded that soon after the crossflow direction is reversed, the plume interior is subjected to vigorous entrainment that quickly erodes the layer structure, essentially eliminating the plume.

The mechanisms of interfacial friction and mixing enable the direct interaction between the interior of the plume and the ambient flow, therefore, the possibility that the vertical flux of momentum associated with entrainment can reduce the shear and thereby limit entrainment must be considered. Several numerical experiments analogous to 13 but with friction and entrainment were performed to examine this possibility. In all cases, explicit mixing resulted in a rapid decrease in the buoyancy of the upper layer. Computation was terminated when the buoyancy in any part of the plume fell below a specified threshold of 0.001 which normally occurred shortly after the current reversal. Of course, the details of these calculations are sensitive to the parametric dependence of the entrainment flux but, since any reasonable form must incor-

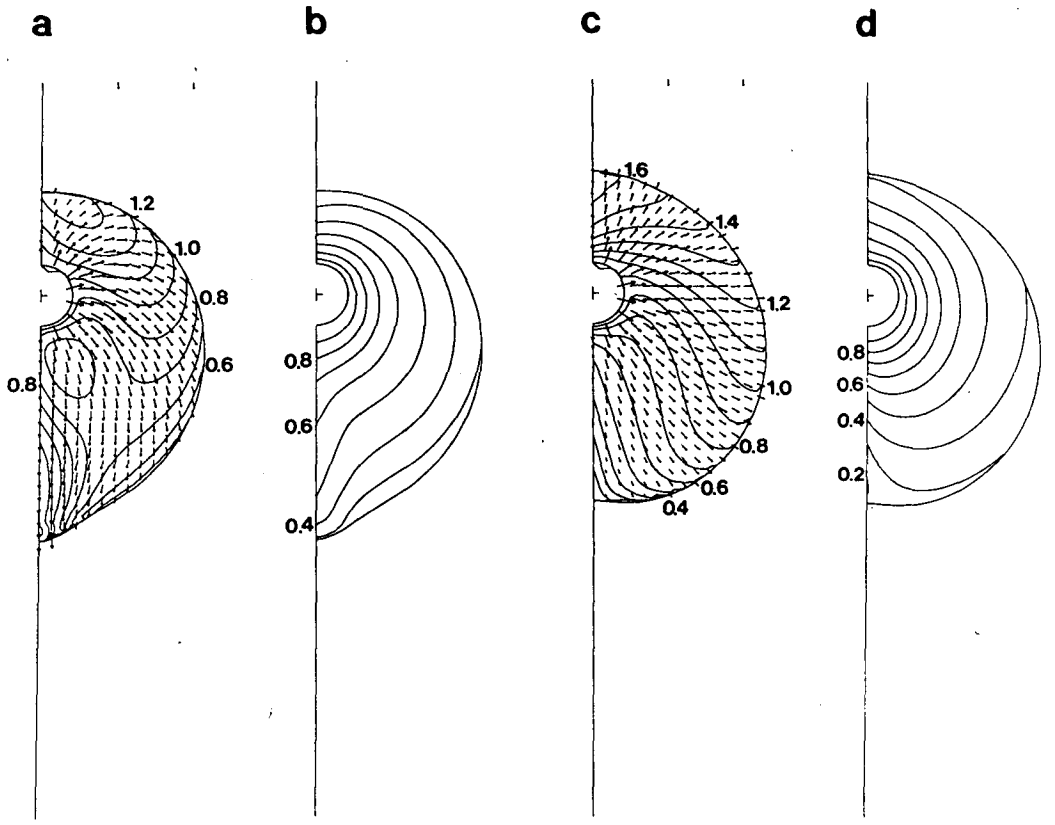

FIG. 12. A comparison of solutions obtained in experiments 11 and 12 at $t = 5.9$. In these experiments, the crossflow velocity was $v_a = -0.5$, the frontal parameters were $F = 1.0$ and $A = -0.1$, and entrainment and friction were allowed with $R_E = R_F = 0.1$. In experiment 11, shown in (a) and (b), the Kelvin number was $R_K = 0.2$ and in experiment 12, $R_K = -0.2$.

porate a rapid rise in entrainment with F_Δ, there is no reason to expect substantially different behavior.

b. *The oscillation of the crossflow direction*

Since the circulation in Long Island Sound is tidal, both the crossflow velocity and the discharge of buoyant fluid from the Connecticut River vary continuously, as in many river plumes; thus, the influence of more gradual changes must be studied.

In experiment 14 the ambient crossflow velocity was specified as $v_a = -\sin(\pi t/10)$ and the discharge transport modulated by 20% using transport $= 1 + 0.2 \cos(2\pi t/10)$, under the assumption that it is proportional to the surface elevation. Using this formulation, $t = 0$ corresponds to low slack water. In addition, friction was neglected because its effect is small and mixing excluded from consideration for simplicity.

The results of calculations for experiment 14, in which $R_E = R_F = 0$ and $R_K = 0.1$ are presented in Fig. 14. The solution at $t = 4.6$, approximately maximum flood, displays the same general features as exhibited by previous solutions for the growth of a plume in a steady crossflow. At $t = 9.6$, approximately high slack water, the rarefaction wave generated by the spreading of the front in the positive y direction (to the left of the source, looking downstream) is evident. The slight peak at the front on the opposite side of the plume is due to the flux convergence produced by the Coriolis acceleration. During the ebb, see the solution at $t = 12.1$, the spread of the front in the negative y direction is slowed causing a surge as in experiment 16. Similarly, a rarefaction is produced where the plume is forced to expand. After a complete cycle, the plume is thin almost everywhere except for the large accumulation to the left of the source in the solution at $t = 20.1$. This is mainly an artifact of the initial conditions adopted. Had the calculation been started at the equivalent of high slack then the accumulation would appear on the other side of the source, modified to some extent by the Coriolis acceleration.

An evaluation of F_Δ during the ebb showed that much of the plume to the right of the source to be subject to vigorous vertical mixing so that only a small area near the source would be likely to survive as a layer. Indeed, in calculations that explicitly included mixing, the upper layer buoyancy became very small soon after the ambient flow reversal. Though this experiment is a poor simulation of the flow in a tidally modulated river plume, it clearly demonstrates that a

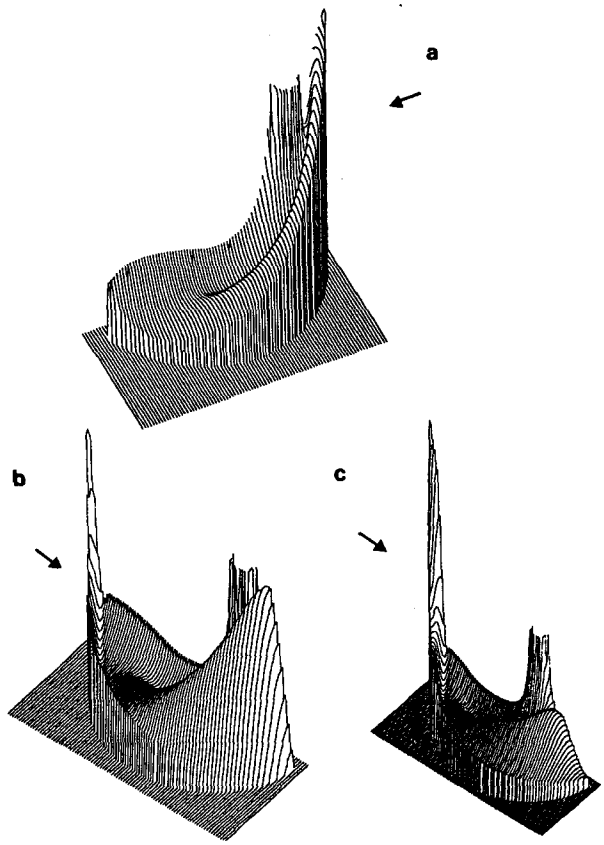

FIG. 13. Surface projections of the layer thickness in experiment 13 at (a) $t = 7.8$, (b) 8.7 and (c) 10.6. No interfacial friction or entrainment were incorporated in this experiment, $R_E = R_F = 0.0$, and the Kelvin number was $R_K = 0.1$. The frontal parameters employed were $F = 1.0$, and $A = 0.0$, and the crossflow velocity was abruptly changed from $v_{a1} = -1.0$ to $v_{a2} = 1.0$ at $t = 8.0$.

plume quickly adjusts to the influence of the crossflow, but once the spreading has been constrained to a particular direction, changing the crossflow velocity results in significant mixing through shear flow instability. The fate of a river plume, it seems, is to be destroyed soon after each turn of the tide and to be reborn and grow on the opposite side of the river mouth.

7. Summary and conclusions

The growth of a buoyant plume from a radially symmetric source was described by Garvine (1984) and the effect of a steady ambient flow in the receiving water was described by O'Donnell (1988). Experiments 1 to 3 investigate the influence of the magnitude of the crossflow velocity on the adjustment and final state of the plume. The results, shown in Fig. 4 and 5, indicate that the primary difference is not in the shape or size of the plume but in the structure of the layer depth distribution. Smaller crossflow velocities allow greater expansion of the buoyant layer which results in an increase of the area subject to the shear instability described by Garvine (1984). Experiments 4 and 5 demonstrate that the structure of the interior flow field is quite sensitive to the value of the parameters A and F that describe mixing and entrainment at the front and therefore better numerical estimates of these must be obtained.

The consequences of the Coriolis effect on the potential for mixing in the plume interior is examined in experiments 6 and 7 and it is shown that a plume is less susceptible to vertical mixing when confined to the shore by both the action of the crossflow and the Coriolis effect. In this situation a boundary current is observed to form approximately one Rossby radius from the source. The associated deepening of the layer overcomes the tendency of the nonrotating plume to become very shallow at the boundary. When the Coriolis effect causes a transport offshore, into the ambient current, the plume thins much more rapidly, presumably resulting in mixing nearshore and the consequent separation of the plume from the coast.

The results of five experiments, 8–12, to assess the consequences of explicit mixing on these results are reported. It is found that at high crossflow velocities the structure of the plume is only mildly modified by mixing since the discharge is rather quickly turned towards the direction of the ambient flow thus minimizing the area of regions of high vertical shear. Mixing has more influence on the structure of the plume at low crossflow velocities, blurring the ring and jump structure that appears as a major feature in the immiscible plume calculations.

The behavior of plumes in time-dependent crossflows are examined in experiments 13 and 14. The response to a sudden change in the direction of the crossflow is calculated to demonstrate the fundamental dynamics of the process. In the absence of mixing, the response of the front is to deepen when the front is slowed, sending a surge into the plume. When it is suddenly accelerated, the layer shoals and a rarefaction propagates towards the source. Of greater significance however, is the result that the bulk shear Froude number becomes large in most of the plume, indicating that intense mixing must occur. Even when the ambient flow is modulated smoothly, as is experienced by the Connecticut River plume in the tidal crossflow of Long Island Sound, calculations indicate that the plume still becomes subject to intense mixing soon after the tidal current changes direction.

In this model, like the others in this series, it is assumed a priori that a strong front surrounds the plume and that it is important to the plume dynamics. Most other models of buoyant discharges and estuarine circulation take the opposite view. Numerical models which employ finite difference methods are unable to resolve these regions of high horizontal gradients because the resolution is limited by computer performance or cost. But, since the experiments discussed here show that the interaction of the plume front and the ambient flow can have major influence on the spread and the mixing of the buoyant water, further

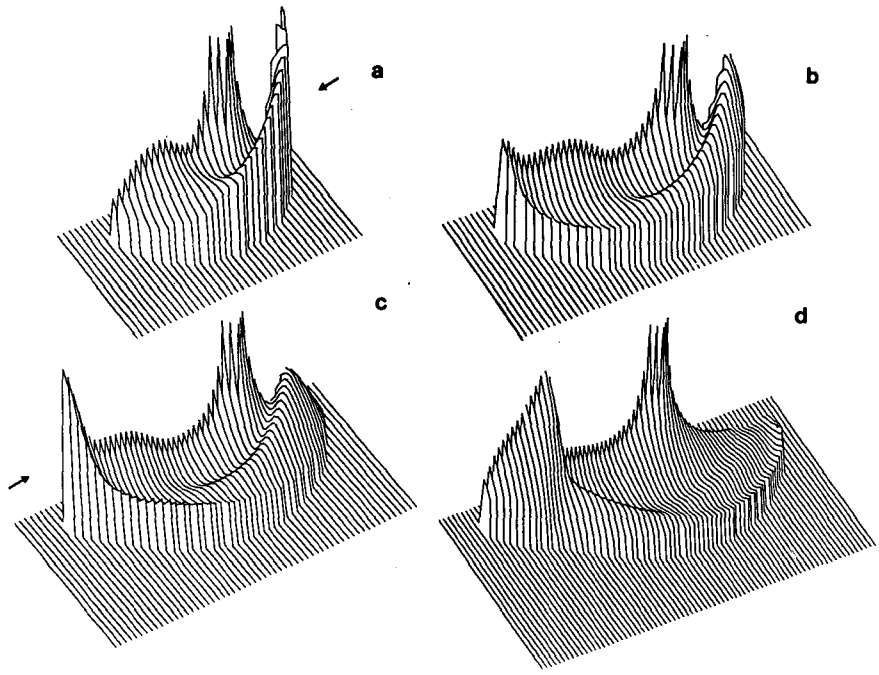

FIG. 14. Surface projections of the interface thickness in experiment 14 at (a) $t = 4.6$, (b) $t = 9.6$, (c) $t = 12.1$, and (d) $t = 20.1$. In this experiment, $R_E = R_F = 0.0$, $R_K = 0.1$, $F = 1.0$ and $A = 0.0$. The crossflow velocity was variable and specified as $v_a(t) = -\sin(t/10)$.

improvement of our understanding and predictive capability for the dispersion of riverborn material requires at least a parameterization of the effect of small scale frontal processes in models of large scale circulation. The clearest example of the potential consequences of frontal dynamics is demonstrated in the results of experiments 13 and 14, which suggest that river plumes may only mix significantly with the underlying ambient fluid at particular phases of the tide but that the mixing occurs over a large area. Thus, the boundary conditions applied in estuarine circulation models may need to be carefully reconsidered.

Acknowledgments. I am grateful to Rich Garvine for his advice, encouragement, and enthusiastic criticism, and to Pablo Huq for permission to use the results of his experiments. This work was supported by grants from the U.S. National Science Foundation, OCE-8315207 and OCE-8816566, and the Natural Environment Research Council of Great Britain.

REFERENCES

Beardsley, R. C., and J. Hart, 1978: A simple theoretical model for the flow of an estuary onto a continental shelf. *J. Geophys. Res.*, **83,** 873–883.

——, R. Limeburner, H. Yu and G. A. Cannon, 1985: Discharge of the Changjiang (Yangtze River) into the East China Sea. *Cont. Shelf Res.*, **4,** 57–76.

Benjamin, T. B., 1968: Gravity currents and related phenomena. *J. Fluid Mech.*, **31,** 209–248.

Boicourt, W. C., 1973: The circulation of water on the continental shelf from Chesapeake Bay to Cape Hatteras. Ph.D. dissertation, The Johns Hopkins University.

Bowman, M. J., and R. L. Iverson, 1977: Estuarine and plume fronts. *Oceanic Fronts and Coastal Processes.* M. J. Bowman and W. E. Esaias, Eds., Springer-Verlag.

Britter, R. E., and J. E. Simpson, 1978: Experiments on the dynamics of a gravity current head. *J. Fluid Mech.*, **88,** 223–240.

Chao, S.-Y., and W. C. Boicourt, 1986: Onset of estuarine plumes. *J. Phys. Oceanogr.*, **16,** 2137–2149.

Ellison, T. H., and J. S. Turner, 1959: Tubulent entrainment in stratified flows. *J. Fluid Mech.*, **6,** 423–448.

Freeman, N. G. S., 1982: Measurement and modeling of freshwater plumes under an ice cover. Ph.D. dissertation, University of Waterloo.

Garvine, R. W., 1974: Physical features of the Connecticut River outflow during high discharge. *J. Geophys. Res.*, **79,** 831–846.

——, 1975: The distribution of salinity and temperature in the Connecticut River estuary. *J. Geophys. Res.*, **82,** 441–454.

——, 1977: Observations of the motion field of the Connecticut River plume. *J. Geophys. Res.*, **82,** 441–454.

——, 1981: Frontal jump conditions for models of shallow buoyant surface layer hydromechanics. *Tellus,* **33,** 301–312.

——, 1982: A steady state model for buoyant surface plumes in coastal waters. *Tellus,* **34,** 293–306.

——, 1984: Radial spreading of buoyant surface plumes in coastal waters. *J. Geophys. Res.*, **89,** 1989–1996.

——, 1987: Estuary plumes and fronts in shelf waters: a layer model. *J. Phys. Oceanogr.*, **17,** 1877–1896.

——, and J. D. Monk, 1974: Frontal structure of a river plume. *J. Geophys. Res.*, **79,** 2251–2259.

Huq, P., 1983: Experimental investigations of tree-dimensional density currents in stratified environments. M.S. Thesis, School of Civil and Environmental Engineering, Cornell University.

Ingram, R. G., 1981: Characteristics of the Great Whale River Plume. *J. Geophys. Res.*, **86,** 2017–2033.

Jirka, G. H., 1982: Turbulent buoyant jets in shallow fluid layers. *Turbulent Jets and Plumes.* W. Rodi, Ed., Pergammon.

Jones, J. M. 1983: Numerical techniques for steady two dimensional transcritical stratified flow problems. Ph.D. dissertation, Cornell University.

Koh, R. C. Y., and L.-N. Fan, 1970: Mathematical models for the prediction of temperature distributions resulting from the discharge of heated water into large bodies of water. USEPA Rep., Water Pollution Control Res. Ser. 16130, DWO 10/70.

Lewis, R. E., 1984: Circulation and mixing in estuary outflows. *Cont. Shelf Res.*, **3**, 201–214.

Luketina, D. A., and J. Imberger, 1987: Characteristics of a surface buoyant jet. *J. Geophys. Res.*, **92**, 5435–5447.

Mayer, D. A., D. V. Hansen and D. A. Ortman, 1979: Long-term current and temperature observations on the middle Atlantic shelf. *J. Geophys. Res.*, **84**(C4), 1176–1792.

O'Donnell, J., 1986: A numerical model of the dynamics of buoyant discharges. Ph.D. dissertation, The University of Delaware, 182 pp.

——, 1988: A numerical technique to incorporate frontal boundaries in two dimensional layer models of ocean dynamic. *J. Phys. Oceanogr.*, **18**, 1584–1600.

——, and R. W. Garvine, 1983: A time dependent, two-layer model of buoyant plume dynamics. *Tellus*, **35A**, 73–80.

Royer, L., and W. J. Emery, 1985: Computer simulation of the Frazer River plume. *J. Mar. Res.*, **43**, 289–306.

Sargent, F. E., 1983: A comparative study of density currents and density wedges. M.S. thesis, Cornell University.

Stolzenbach, K. D., and D. R. F. Harleman, 1971: An analytical and experimental investigation of surface discharges of heated water. Tech. Rep. 135, Parsons Lab., Massachusetts Institute of Technology, Cambridge, MA.

Stronach, J. A., 1977: Observation and modeling studies of the Frazer River plume. Ph.D. Dissertation, University of British Columbia.

Turner, J. S., 1973: *Buoyancy Effects in Fluids.* Cambridge University Press.

Wiseman, W. J., L. D. Wright, L. J. Rouse and J. M. Coleman, 1976: Periodic phenomena at the mouth of the Mississippi River. *Contrib. Mar. Sci.*, **20**, 11–32.

Wright, L. D., and J. M. Coleman, 1971: Effluent expansion and interfacial mixing in the presence of a salt wedge, Mississippi River delta. *J. Geophys. Res.*, **76**(36), 8649–8661.

Zhang, Q. H., G. S. Janowitz and L. J. Pietrafesa, 1987: The interaction of estuarine and shelf waters: a model and applications. *J. Phys. Oceanogr.*, **17**, 455–469.